*Progress In Electromagnetics Research B, Vol. 32, 91–106, 2011*

# AN INNOVATIVE RADAR IMAGING SYSTEM BASED ON THE CAPABILITY OF AN UWB ARRAY TO STEER SUCCESSIVELY IN DIFFERENT DIRECTIONS

**L. Desrumaux[1], M. Lalande[1,*], J. Andrieu[1], V. Bertrand[2], and B. Jecko[1]**

[1]XLIM/OSA, IUT GEII, 7 rue Jules Vallès, Brive 19100, France

[2]CISTEME, ESTER, B. P. 6913, Limoges Cedex 87069, France

**Abstract**—An innovative radar imaging system, based on the capability of a fixed UWB array to radiate short pulses in different directions along time with the principle of electronic beam steering, is presented in this paper. To demonstrate its concept, the analysis presented in this paper is based on simulation results. As function of the use of either only one antenna or several antennas in reception, two radar imaging algorithms have been developed and are detailed in this paper. These algorithms permit to obtain an image of the analyzed scene thanks to the transient beam pattern of the array used in emission. Finally, with a same analyzed scene, these algorithms have been compared with the time reversal method and the back projection algorithm, in association with a SAR imaging system. The conditions of applicability of these methods are also discussed.

## 1. INTRODUCTION

In recent years, investigations directed to the realization of Ultra Wide Band (UWB) systems that radiate transient waveforms and exhibit operating bandwidths of over one decade are made intensively in many countries. Such systems make possible the radiation of very short pulses, having a rise time of around 100 ps and a time duration lower than one nanosecond. These radiated waveforms make them interesting for many applications such as transient radar cross section (RCS) measurements [1] and UWB synthetic aperture Radar (SAR) systems [2, 3]. The main interest of such systems is that the radar resolution is proportional to the radiated bandwidth. Contrary

*Received 30 May 2011, Accepted 2 July 2011, Scheduled 8 July 2011*

* Corresponding author: Michele Lalande (lalande@brive.unilim.fr).

to narrow band systems, a second advantage is the capability of identifying stealth targets.

This paper presents, from simulation results obtained with the CST Microwave Studio software, two radar imaging algorithms allowing the detection of multiple targets with the use of an Ultra Wide Band (UWB) antenna array. These algorithms are associated with the capability of a Radar system to steer electronically in different directions, azimuth per azimuth, successively along time. Contrary to the back projection algorithm [4, 5] or the time reversal method [6, 7], respectively associated with a SAR configuration or with the use of many sensors in reception, these algorithms permit to get an image of the analyzed scene by adjusting the time delays between the feedings of each antenna, with the use of the transient beam pattern of the fixed array (Fig. 1).

Figure 1 shows that the transient beam pattern of an array, composed of 5 antennas in this case, has the shape of an octopus with 5 tentacles. In the case of a simultaneous feeding of the antennas,

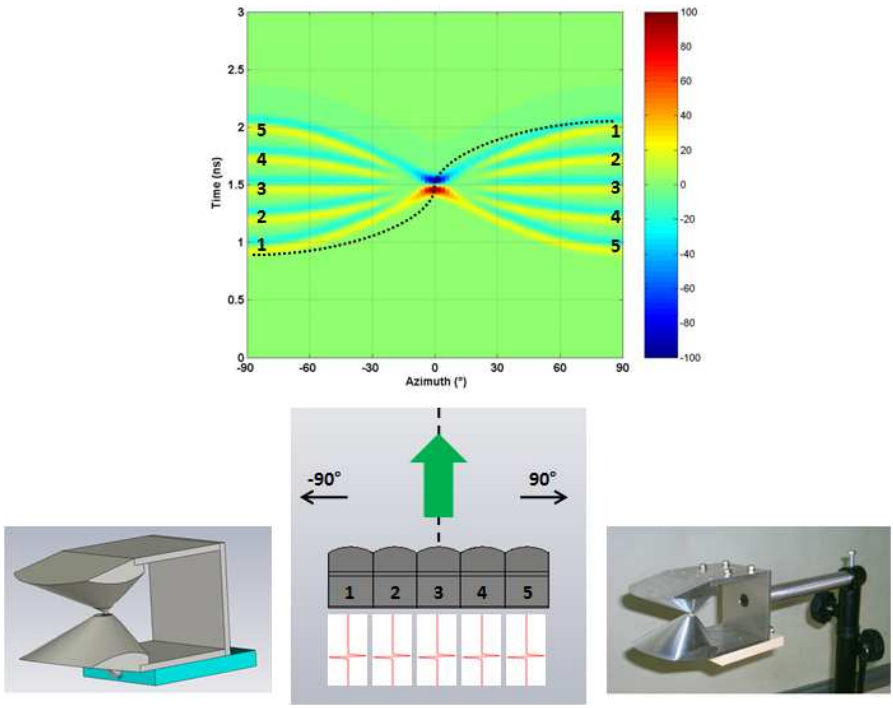


**Figure 1.** The transient beam pattern of an array composed of 5 *Shark* antennas.

the accumulation of power is reached at the azimuth 0°, defined as the heart of the octopus, and each tentacle corresponds to the contribution of one antenna. Conversely to the case of the antenna number 5, the pulse radiated by the antenna number 1 is the first to reach the azimuth −90° and is the last to reach the azimuth +90°. In the configuration presented on this figure, the elementary antenna used in the simulation is the *Shark* antenna [8, 9], working in the frequency band [800 MHz–8 GHz]. The width of each monocycle feeding pulse, allowing the limitation of the coupling between the antennas [10], is 300 ps.

In this paper, Section 2 is dedicated to the presentation of both the UWB array and the analyzed scene. Then, Section 3 and Section 4 will focus on two Radar imaging algorithms, with a reception configuration including respectively only one sensor and several sensors. Finally, in Section 5, the results and the conditions of applicability of these algorithms are discussed and compared with the back projection algorithm and the time reversal method.

## 2. THE ANALYZED SCENE

Figure 2 presents the configuration of the analyzed scene and the Radar system used, simulated with the CST Microwave Studio software:

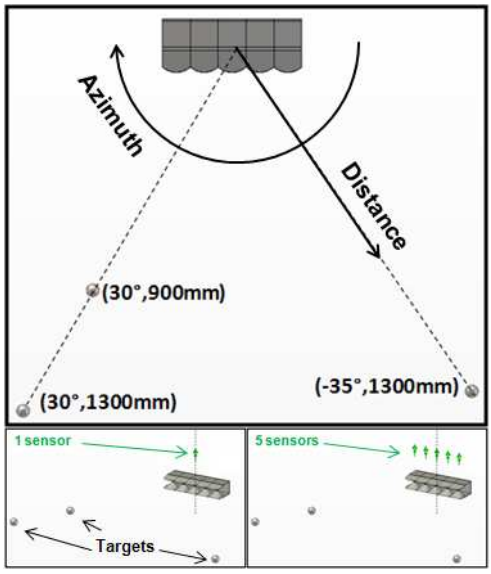


**Figure 2.** The configuration of the analyzed scene.

- The analyzed scene is composed of three spherical targets, with a diameter of 60 mm, situated in three different locations (azimuth, distance) from the Radar: (30°; 900 mm), (30°; 1300 mm), and (−35°; 1300 mm). Thus, two targets have been positioned at a same azimuth and two targets have been positioned at a similar distance from the Radar.
- The Emission module of the Radar is set up with an array of 5 *Shark* antennas. In order to scan a wide area, from the azimuth −55° to the azimuth +55° with a 5° step, time delays have been applied between the feeding pulses of the antennas to steer the radiated fields in each wanted direction. Thus, 23 shots have been necessary to scan the area in front of the Radar.
- Concerning the Reception module of the Radar, Fig. 2 shows that two configurations have been envisaged. The first one includes only one sensor, located above the central antenna of the array and the second one includes several sensors, each of them being located above one antenna of the array (one sensor in reception per antenna in emission).

## 3. RADAR IMAGING ALGORITHM WITH ONE SENSOR

With the reception configuration composed of only one sensor, the principle of the Radar imaging algorithm is to sum the radiated fields belonging to the tentacles of the transient beam pattern of the array, by analogy with the back projection algorithm for which the concept is to sum the values belonging to an hyperbola. In this configuration, contrary to the SAR one, the Radar does not need to move along the analyzed scene because it is based on the capability of the array to steer electronically in different directions.

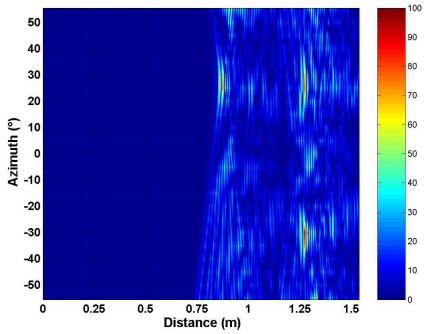


**Figure 3.** Responses of the three targets.

As the scene has been scanned with 23 shots, radiated in different directions thanks to the control of time delays on the feeding pulses, the map representing the responses of the targets, as function of distance along the horizontal axis and azimuth along the vertical axis [11], is shown in Fig. 3. It clearly displays an "octopus" with 5 tentacles for each of them.

From this map, the idea consists in isolating the different "octopuses" and particularly their heart, corresponding to the location of a target. It can be realized in different steps:

1) Firstly, the maximum level of this map is searched and all the values belonging to the tentacles, for which this maximum level is the heart, are summed. Fig. 4 indicates the analytical method permitting to collect the values belonging to these tentacles, thanks to the distance d between the feedings of two adjacent antennas in the array.
As represented in Fig. 4, the maximum level identified on the map corresponds to an azimuth defined as $\theta_{\text{Heart}}$. From this azimuth, the values belonging to the corresponding octopus are collected for all the other azimuths $\theta$, and are then summed. However, the sum of these values must take into account some weighting coefficients. Indeed, if the steering angle moves away from the azimuth 0°, the level of the radiated field will decrease [12], and this phenomenon will have to be compensated. Moreover, if the considered azimuth $\theta$ moves away from the heart of the octopus, the level of the associated field along the tentacles will also decrease. As a result, from the identified level of the heart, the level of the tentacles can be obtained thanks to a weighting matrix (Fig. 5) for each azimuth $\theta$. This matrix, which only depends on the configuration of the array used in emission, is the result of

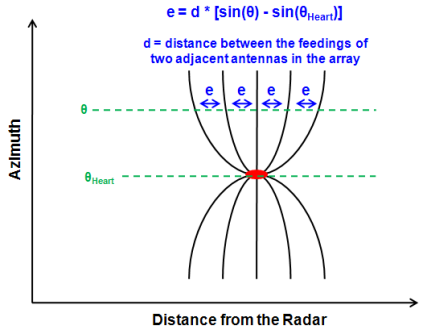


**Figure 4.** Recovery of the values belonging to an octopus.

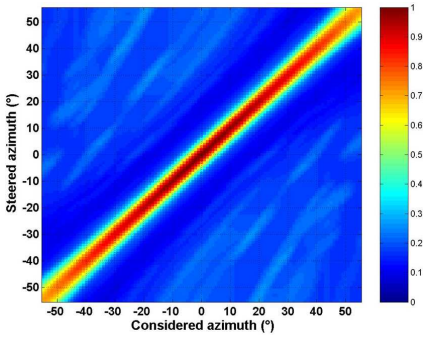


**Figure 5.** Weighting matrix.

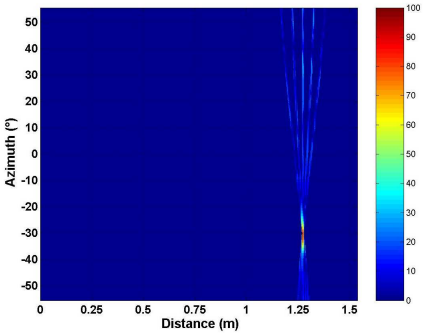


**Figure 6.** Octopus corresponding to the maximum level of the responses.

23 simulations (one simulation per steered azimuth). It has been obtained in evaluating the level of the radiated fields all around the array (represented along the horizontal axis of Fig. 5) for all the steered azimuths (represented along the vertical axis of Fig. 5). For example, with a weighting coefficient equal to 1, this matrix shows that the maximum level of the radiated field is obtained at the azimuth 0° when the steered azimuth is 0°. Besides, the diagonal illustrates the fact that the radiated field decreases with the moving away of the steered azimuth from the central one.

2) Then, after having saved the sum of the values belonging to the tentacles (Fig. 6) in an imaging matrix, thanks to the weighting coefficients, the considered octopus is removed from the map representing the responses of the targets (Fig. 7). Indeed, because of the removal of the octopus presented in Fig. 6, the maximum level of the map displayed in Fig. 7 is around 80 while it is equal to 100 on the initial map (Fig. 4).
3) From this lightened matrix, the two previous steps are repeated until the matrix of responses is blank. Thus, for each iteration, the octopus corresponding to the maximum level of the new matrix of responses is removed and the sum of this octopus is added in the imaging matrix. Finally, this whole imaging matrix represents the image of the scene, normalized at 100% for the maximum value (Fig. 8).

On the imaging matrix, the locations of the targets are represented with the highest levels, encircled in yellow. Thanks to the weighting matrix, the contributions of each target have been correctly identified.

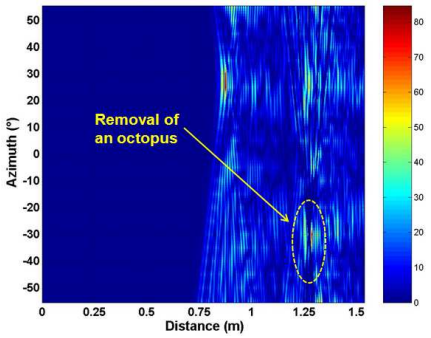


**Figure 7.** Lightened responses of the targets.

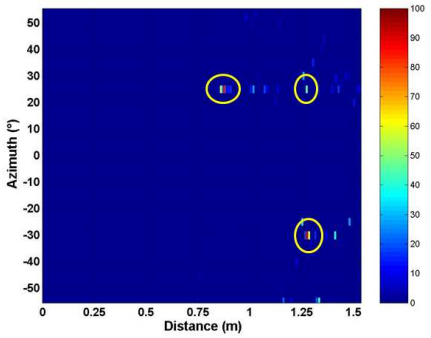


**Figure 8.** Imaging matrix (gathering of the sums of the octopuses).

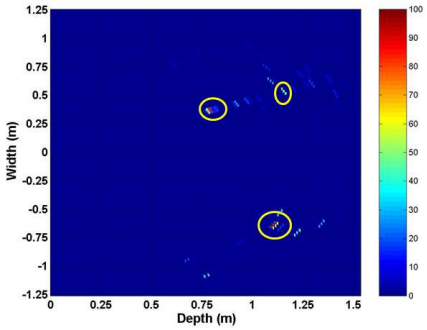


**Figure 9.** Final representation of the imaging matrix (Cartesian coordinates).

Indeed, if the weighting matrix had not been used, one of the two target contributions, located at a same distance of 1300 mm from the Radar, would have disappeared with the subtraction operation.

To compare this imaging matrix with the scene represented in Fig. 2, the coordinates have been modified (Fig. 9) to display the image of the analyzed scene as function of width and depth (Cartesian coordinates) instead of azimuth and distance (Polar coordinates).

This figure shows some interferences but they are not high enough to be considered as target contributions.

With this reception configuration, it is important to notice that the developed algorithm is very different from a classical search of maxima, for which a target position would be associated with each maximum value found, for the following reasons:

- The correspondence between one maximum value and one target does not permit to solve the problem of detection because the number of targets on the scene is unknown. In this case, for example, it would be necessary to know that there are three targets before searching the first three corresponding maximum values.
- The main reason why it is not a solution to consider one maximum value as a target position is that some interferences will appear if two targets are very close. Indeed, if they are high enough, these interferences will wrongly be considered as a target position. For example, Fig. 3 shows an interference, between the two targets located at a distance of 1300 mm from the Radar, that could have been considered as a fourth target, while it is not the case. Thanks to the developed algorithm and the successive subtractions of the octopuses, this interference has disappeared along the iterations and it is finally more difficult to consider it as a target position.

## 4. RADAR IMAGING ALGORITHM WITH SEVERAL SENSORS

With the reception configuration composed of several sensors, the Radar imaging algorithm developed is based on the Digital Beam Forming (DBF) method [13, 14]. Its principle consists in applying numerical time delays on the received signals to make them focus on a particular direction. As a result, if an aimed direction is the one of a target, the signals received on the sensors will be synchronized and the signal to noise ratio will increase. Conversely, if the aimed direction does not correspond to the location of a target, no useful information will be obtained.

In this section, the analyzed scene is the same as the one analyzed in Section 3, but the reception configuration is composed of 5 sensors have been considered instead of one (Fig. 10). In that case, the sensor number 1 will be the first to receive the contribution of a target located at the azimuth $-35°$ while the sensor number 5 will be the

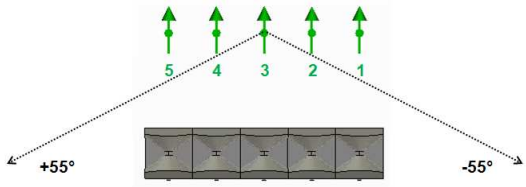


**Figure 10.** Reception configuration with 5 sensors.

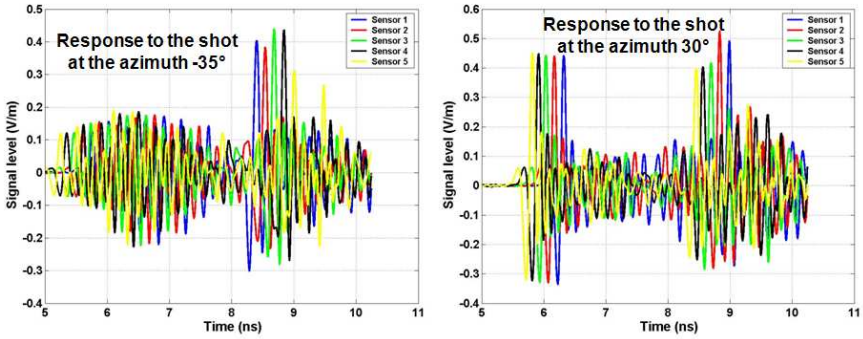


**Figure 11.** Signals received on the five sensors in the directions of the targets.

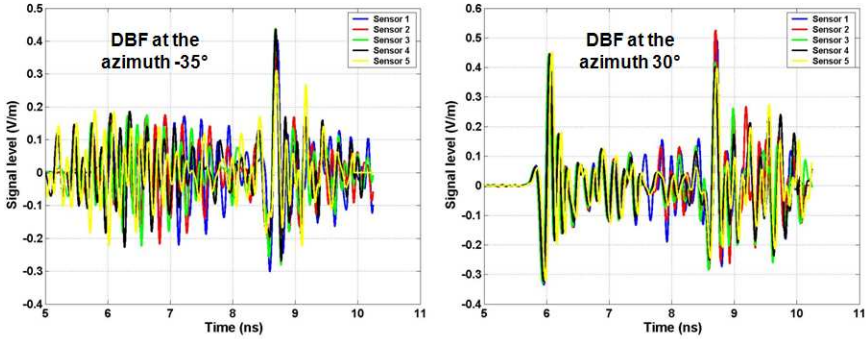


**Figure 12.** Application of time delays on the sensor responses.

last. Conversely, the sensor number 5 will be the first to receive the contribution of a target located at the azimuth 30° while the sensor number 1 will be the last. This phenomenon can clearly be seen in Fig. 11, which displays the responses to the shots at the azimuths −35° and 30° on the five different sensors.

From these received signals, the time delays between them is adjusted to focus on their direction of origin (Fig. 12). For each considered direction, the useful signal is obtained with the addition of these five adjusted contributions, which involves an increase of the signal to noise ratio (Fig. 13).

Executing this operation for all the directions for which a shot has been done, this method permits to get the map displayed in Fig. 14 and in Fig. 15, respectively in Polar coordinates (representation as function of azimuth and distance) and in Cartesian coordinates (representation as function of width and depth).

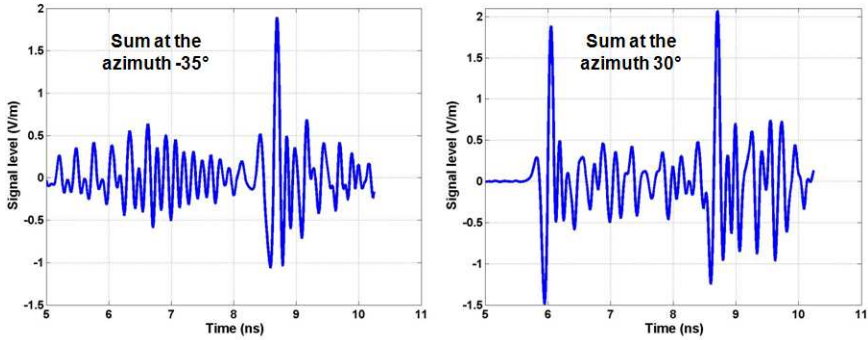


**Figure 13.** Final signal relative to a particular direction.

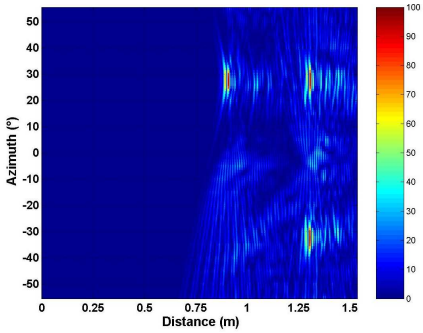


**Figure 14.** Imaging matrix (Polar coordinates).

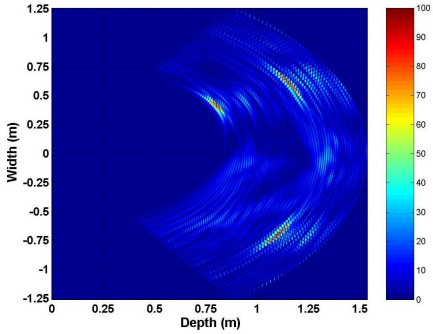


**Figure 15.** Imaging matrix (Cartesian coordinates).

These figures show that the target locations are clearly identified and that the interferences of Fig. 3 have disappeared. It can be noted that higher is the number of sensors better is the quality of the image, thanks to a higher increase of the signal to noise ratio.

## 5. COMPARISON OF DIFFERENT METHODS AND ALGORITHMS

The main of this section is the comparison of the two Radar imaging algorithms developed in Section 3 and in Section 4. Associated with the capability of the array used in emission to steer successively in different directions along time, these algorithms are also compared with the back projection algorithm associated with a SAR imaging

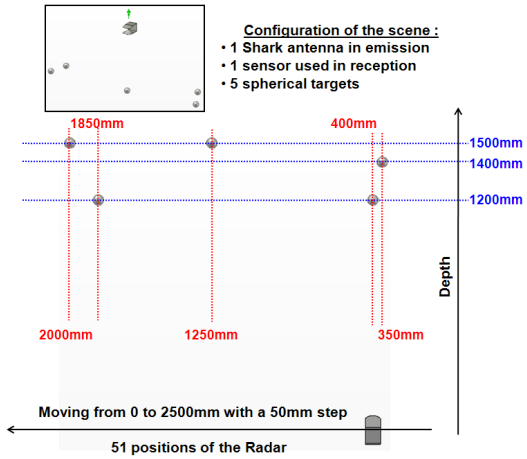


**Figure 16.** Scene analyzed in a SAR configuration.

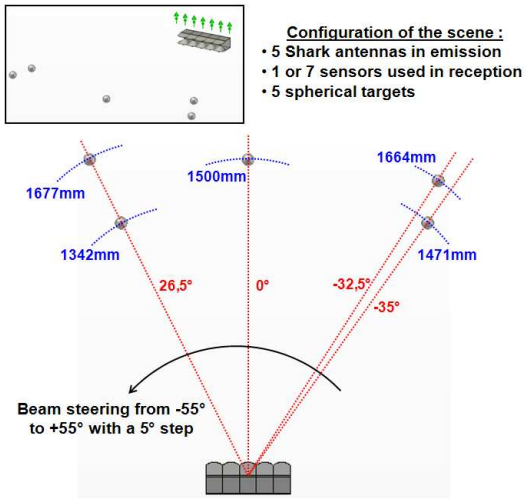


**Figure 17.** Scene analyzed in an electronic beam steering configuration.

system and the time reversal method associated with the use of many sensors in reception.

For this study, the same scene has been analyzed and a higher number of targets has been considered (five instead of three). Fig. 16 presents the analyzed scene with the principle of SAR imaging and Fig. 17 presents the same scene with the principle of electronic

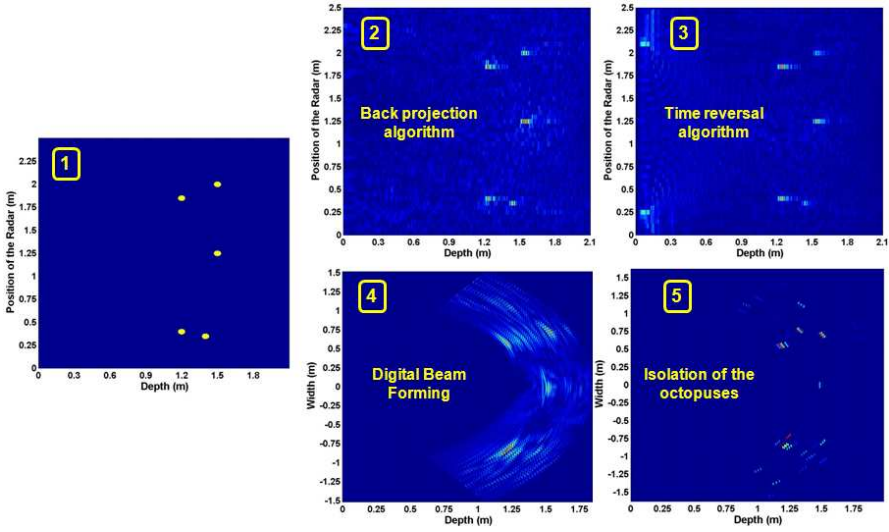


**Figure 18.** Comparison of 4 radar imaging algorithms.

beam steering in emission. In the SAR configuration, 51 shots have been realized while there have been 23 shots in the beam steering configuration.

The results of these two analysis are presented in Fig. 18, with the use of two different algorithms per method:

- Panel 1 shows the analyzed scene with an adapted scale.
- Panel 2 displays the result of the back projection algorithm, in association with the SAR imaging method.
- Panel 3 displays the result of the time reversal algorithm, in association with the SAR imaging method, equivalent in this case to the use of several sensors in reception.
- Panel 4 displays the result of the algorithm developed in Section 3, with the use of only one sensor in reception, consecutively to 23 shots in different directions.
- Panel 5 displays the result of the Digital Beam Forming algorithm developed in Section 4, with 7 sensors in reception, consecutively to 23 shots in different directions.

This figure allows the following comments:

- The four developed algorithms permit to get a relatively clear detection of each target.

- With the back projection algorithm, thanks to the addition of the values belonging to an hyperbola, the contributions of each target is clearly identified and the interferences between the echoes of two different targets are insignificant (Panel 2). Moreover, the time duration of this algorithm is very short (around 9 s in this case). As a result, this algorithm is simple and effective. However, the drawback of this algorithm is its association with a SAR method, for which involves the fact that the Radar has to move along the analyzed scene. In the case where the system has to be discreet, this necessary moving could be a weakness.
- Concerning the time reversal method, the SAR configuration has permitted to make an analogy with the use of many sensors positioned along the scene. Panel 3 shows that the resulting image is obtained with a high precision but two drawbacks can be identified: the signal processing is relatively complex and its time duration is quite long (around 43 minutes in this case).
- Consecutively to the electronic beam steering realized by the fixed Radar in emission, the first proposed algorithm is the one developed in Section 3. It consists in isolating the successive octopuses relative to a high level, defined as its heart. With this principle, only one sensor is needed in reception to make possible the detection of the targets. Panel 4 shows that the targets have correctly been located, in spite of the existence of some interferences, having a low level. However, even if the level of these interferences is low, these ones are probably too many to permit a clear identification of the real targets. Thus, this phenomenon indicates a limitation of this algorithm: if the number of targets is too high and/or they are too close to each other, the effectiveness of this algorithm will decrease. Indeed, in these cases, a high interference between two targets could be considered as the heart of an octopus and could involve the subtraction of an useful information that would permit to locate a real target.
- As far as the Digital Beam Forming is concerned, with the use of 7 sensors in reception, Panel 5 shows that the highest levels of the responses are located at the coordinates of the 5 targets. Indeed, contrary to Panel 4, for which some echoes do not correspond to real targets, all the echoes of panel 5 correspond to the real ones. This method is then less sensitive to interferences. However, it can be noted that the targets echoes are larger than the ones of the other panels. This lack of precision is due to the change in coordinates (from Polar coordinates to Cartesian ones), which can clearly be seen in Section 4 with the passage from Fig. 14 to Fig. 15. Indeed, with an angular step of 5°, the discretization

involved by the beam steering configuration is 105 mm and 131 mm respectively for depths of 1200 mm and 1500 mm, whereas the discretization is equal to 50 mm with a SAR configuration. Thanks to the increase of the signal to noise ratio with the increase of the number of sensors, the interferences between the targets have been attenuated. As a result, few detection errors are possible. In spite of its simplicity, the main drawback of this algorithm is the use of several sensors to be the most efficient as possible.

These results permits to deduce these comments:

- In the case of the use of the SAR imaging method, with a not too disruptive environment, it is more judicious to execute the back projection algorithm than the time reversal algorithm because, for a similar result, it is more simple and has a shorter time duration.
- In the case of the electronic beam steering with a fixed Radar, the best signal processing is the one using the Digital beam Forming principle, even if the number of sensors can be high. Indeed, this algorithm is less sensitive to the noise and to the interferences than the one consisting in isolating the octopuses.

## 6. CONCLUSION

In comparison with two existing algorithms associated with a SAR configuration, two algorithms have been presented in this paper in association with the principle of electronic beam steering in emission. The same simulated scene has been considered to identify the advantages and the drawbacks of each Radar imaging algorithm.

The first presented algorithm, inspired by the back projection algorithm, is based on the sum of the radiated fields belonging to the tentacles of the transient beam pattern of an UWB array. It needs only one sensor in reception to be applied. The second one uses the principle of Digital Beam Forming in reception, involving the increase of the signal to noise ratio with the increase of the number of sensors. With the development of these algorithms, the contributions of several targets have been distinguished, in spite of their location at a same depth from the Radar, with a different azimuth, or at a same azimuth with a different depth. The main advantage of such a method, including an electronic beam steering in emission and an adequate signal processing in reception, is that the system is fixed and discreet. Indeed, the time duration of the analysis of a scene is very short because, contrary to the SAR configuration, it is not necessary to move the system along the scene.

As the algorithms presented in this paper are consecutive to simulation results, future works will consist in applying these methods to detect the positions of several targets inside an experimental context.

## REFERENCES

1. Immoreev, I. I. and J. D. Taylor, "Optimal short pulse ultra-wideband radar signal detection," *Ultra-wideband Short-pulse Electromagnetics 5*, Smith and Cloude (eds.), 207–214, Kluwer Academic/Plenium Publishers, 2002.
2. Ressler, M. A., "The army research laboratory ultra wideband BoomSAR," *Geoscience and Remote Sensing Symposium*, Vol. 3, 1886–1888, 1996.
3. Boutros, J. and G. Barrie, "Ultra-wideband synthetic aperture radar imaging, effect of off-track motion on resolution," *Technical Memorandum*, Nov. 2003.
4. Barrie, G., "Through-wall synthetic aperture radar (TWSAR) 3D imaging, algorithm design," *Technical Memorandum*, Nov. 2004.
5. Ahmad, F., M. G. Amin, and S. A. Kassam, "Synthetic aperture beamformer for imaging through a dielectric wall," *IEEE Transactions on Aerospace and Electronics Systems*, Vol. 41, No. 1, Jan. 2005.
6. Fink, M., C. Prada, D. Cassereau, and E. Kerbrat, "Time reversal techniques in non destructive testing," *Europ. Cong. Acoust.*, 2002.
7. Neyrat, M., C. Guiffaut, and A. Reinex, "Reverse time migration algorithm for detection of buried objects in time domain," *Antennas and Propagations Society International Symposium*, Jul. 2008.
8. Desrumaux, L., A. Godard, M. Lalande, V. Bertrand, J. Andrieu, and B. Jecko, "An original antenna for transient high power UWB arrays: The *Shark* antenna," *IEEE Transactions on Antennas and Propagation*, Vol. 58, No. 8, 2010.
9. Desrumaux, L., M. Lalande, J. Andrieu, V. Bertrand, and B. Jecko, "The Shark antenna: A miniature antenna for transient ultra wide band applications in the frequency band 800 MHz–8 GHz," *European Conference on Antennas and Propagation EUCAP 2010*, Barcelona, Spain, Apr. 2010.
10. Lalande, M., J. C. Diot, S. Vauchamp, J. Andrieu, V. Bertrand, B. Beillard, B. Vergne, V. Couderc, A. Barthélémy, D. Gontier, R. Guillerey, and M. Brishoual, "An ultra wideband impulse

optoelectronic radar: RUGBI," *Progress In Electromagnetics Research B*, Vol. 11, 205–222, 2009.

11. Salo, G. R. and J. S. Gwynne, "UWB antenna characterization and optimization methodologies," *Ultra-wideband Short-pulse Electromagnetics 6*, Mokole, et al. (eds.), 329–336, Kluwer Academic/Plenium Publishers, 2003.
12. Desrumaux, L., S. Vauchamp, V. Bertrand, V. Couderc, M. Lalande, and J. Andrieu, "Transient measurements of an agile UWB array," *European Microwave Week 2010*, Paris, Sep. 2010.
13. Hum, S. V., H. L. P. A. Madanayake, and L. T. Bruton, "UWB beamforming using 2-D beam digital filters," *IEEE Transactions on Antennas and Propagation*, Vol. 57, No. 3, 807–807, Mar. 2009.
14. Schuler, K. and W. Wiesbeck, "Tapering of multitransmit digital beamforming arrays," *IEEE Transactions on Antennas and Propagation*, Vol. 56, No. 7, Jul. 2008.